Int. J. Electrochem. Sci., 14 **(2019)** 59 – 74, doi: 10.20964/2019.01.24

International Journal of
ELECTROCHEMICAL
SCIENCE
www.electrochemsci.org

Influence of Storage Temperature on the Corrosion Behavior of Tinplate in Citric Acid Solution

Jihui Wang[1,2,*] , *Li Zhang*[1,2], *Yun Gao*[2], *Xin Liu*[2], *Wenbin Hu*[2]

[1] State Key Laboratory of Hydraulic Engineering Simulation and Safety, Tianjin University, Tianjin 300350, P R China
[2] Tianjin Key Laboratory of Composite and Functional Materials, School of Materials Science and Engineering, Tianjin University, Tianjin 300350, P R China
*E-mail: jhwang@tju.edu.cn

Received: 6 August 2018 / *Accepted:* 4 October 2018 / *Published:* 30 November 2018

The influence of storage temperature on the corrosion behavior of tinplate was investigated in 0.1mol/L citric acid solution by using immersion test, polarization curve and electrochemical impedance spectroscopy (EIS). The surface morphology of tinplate before and after corrosion was characterized by scanning electron microscopy (SEM), and the dissolution content of iron and tin ions in citric acid solution was determined by inductively coupled plasma mass spectrometer (ICP-MS). The experimental results show that with the increasing of storage temperature the corrosion potential of tinplate in citric acid solution is shifted negatively whereas the corrosion current density is increased obviously. EIS spectrum of tinplate in citric acid solution is transferred from two time constants at the initial immersion into one time constant with the prolonging of immersion time, and the radius of capacitive arc is decreased with the increasing of storage temperature. Meanwhile, the dissolution rate of tin and iron in citric acid is also promoted by storage temperature. Finally the corrosion mechanism of tinplate in citric acid solution is proposed and discussed, and the activation energy is calculated and correlated with the corrosion process of tinplate.

Keywords: storage temperature; tinplate; citric acid; corrosion behavior; EIS spectrum

1. INTRODUCTION

Tinplate is a cold-rolled low carbon steel sheet with tin plated on both sides, and extensively applied as main packaging material in canning industry for sealing food and beverage because of its excellent formability, solderability and corrosion resistance with good appearance of tin [1-3]. However, corrosion problems such as pitting perforation, loss of seal integrity, discoloration and food pollution by tinplate's corrosion are often occurred [4-6]. So it's essential to explore the corrosion behavior and mechanism of tinplate in canning environments so as to guarantee the quality of food and beverage.

The corrosion behavior of tinplate depends many factors including can material (composition, surface morphology, grain size, plastic deformation, base steel, etc.), kinds of contacting medium (food and beverage matrix, acidity, presence of complexing agents) and storage conditions (vacuum degree, duration, environmental humidity, temperature, air permeability)[3, 7]. The corrosion behavior of tinplate containers in brine and pickled sauce with seafood was investigated at room temperature by using polarization curve and EIS experiments, and the degradation degree was evaluated by the variation of electrochemical parameters during the storage duration [4, 6]. The corrosion properties of tinplate in sodium chloride solution [8-12], citric acid solution [7, 9, 11, 13], industrial water [14], functional beverage [15] and coffee drinks [16] were also determined at room temperature, and the corrosion mechanism was proposed and discussed.

Canned food and beverage are normally placed in refrigerator (cold), normal or higher temperature environment, which has an important influence on its storage life because of the different dissolution rate of tin into canned food. In a survey of canned US military rations, the tin content of five types of fruit in unlacquered cans at 37 ^{o}C after 20 months was 12 times higher than that at 1 ^{o}C (420 and 34 mg/kg, respectively). For seven types of mixed dishes in unlacquered cans the tin content at 37 ^{o}C was 6 times higher than that at 1 ^{o}C (190 and 32 mg/kg, respectively) [3, 17]. In 0.1mol/L NaCl solution, the corrosion behavior of tinplate was investigated under different storage temperature, and the corrosion mechanism was discussed [18]. However, until now there are few reports done about the corrosion of tinplate in citric acid solution under different storage temperature.

In order to explore the effectiveness of packaging cans in fruit beverage and citric acid containing food, the corrosion behavior of tinplate in 0.1mol/L citric acid solution was investigated in this work under different storage temperature by using polarization curve, electrochemical impedance spectroscopy (EIS) and immersion test. The morphology of corroded tinplate was observed by scanning electron microscopy, and the dissolution content of Fe and Sn elements in citric acid solution was also determined. And then the activation energy of tinplate in citric acid solution was calculated, and the effect of temperature on the corrosion process of tinplate was proposed and discussed.

2. EXPERIMENTAL

2.1 Material

Tinplate sheet used in this work is composed by a low carbon steel substrate with the thickness of 0.4 mm and tin coating with the nominal weight of 2.8 g/m^2 on both sides of steel by electrodeposition method. After reflowing at 250°C and electrochemical passivation in sodium chromate solution, the tinplate samples with the dimension of 60 mm×60 mm and surface roughness of 0.33 μm were degreased by ethanol and dried before exposed to citric acid solution.

2.2 Electrochemical measurements

The polarization curve and electrochemical impedance spectroscopy (EIS) of tinplate in 0.1 mol/L citric acid solution at the temperature of 5 ^{o}C, 20 ^{o}C and 37 ^{o}C were carried out in an electrolytic cell by using Autolab 302N electrochemical workstation. A three-electrode system with the tinplate by a exposed area of 19.6 cm^2 as working electrode (WE), a saturated calomel electrode as reference electrode (RE) and a ruthenium-titanium electrode as counter electrode (CE) was used. The testing temperatures of 5 ^{o}C, 20 ^{o}C and 37 ^{o}C were obtained by using biochemical incubator in order to simulate the different storage temperature during the transportation and storage process of canned food.

After 30 minutes' immersion, the polarization curve of tinplate in citric acid solution was conducted at a scan rate of 0.1667 mV/s, and the corrosion potential E_{corr} and corrosion current density I_{corr} were calculated and obtained. EIS measurements were acquired under the immersion time of 3, 6, 12, 24, 120, 240, 480 and 720 hours at the open circuit potential with a 10 mV amplitude signal and the applied frequency ranging from 100 kHz to 0.01 Hz. The measured EIS spectrum was then analyzed in term of appropriate equivalent circuits by applying ZsimpWin software, and then the electrochemical fitting parameters were determined by the simulation.

2.3 Immersion test

Tinplate samples with the dimension of 60 mm×60 mm were immersed in 0.1 mol/L citric acid solution at the temperature of 5 ^{o}C, 20 ^{o}C and 37 ^{o}C for 30 days. After immersion times of 24, 240, 480 and 720 hours, the corroded samples were taken out from the solution and then cleaned with distilled water and ethanol. The corroded surface of tinplate was observed by scanning electron microscopy, and the composition of corroded surface was analyzed by EDS Genesis XM2 energy dispersion spectroscopy.

Meanwhile, 1mL solution was collected from the immersion electrolyte after immersion time of 6, 12, 24, 120, 240, 480 and 720 hours, and the concentration of Fe and Sn dissolved in the solution was measured by using Agilent 7700x inductively coupled plasma mass spectrometry (ICP-MS).

3. RESULTS

3.1 Polarization curve

The polarization curve of tinplate in 0.1 mol/L citric acid at different temperatures is shown in Fig. 1. It can be observed from Fig.1 that with the increasing of storage temperature the corrosion potential of tinplate is shifted negatively from -0.511 V (5 ^{o}C) to -0.541V (20 ^{o}C) and -0.547 V (37 ^{o}C). Meanwhile there is a passive region occurred in the anodic polarization curve especially at temperature of 20 ^{o}C and 37 ^{o}C, and the initiating passive potential (-0.490 V at 20 ^{o}C and -0.502V at 37 ^{o}C) and transpassive potential (-0.340V at 5 ^{o}C, -0.420 V at 20 ^{o}C and -0.432V at 37 ^{o}C) of tinplate are decreased with the increasing of temperature (Fig.1). This passive state of tinplate in citric acid solution is caused by the anodic dissolution of tin and the formation of insoluble thin film of $Sn(OH)_4$ and SnO_2 under the reaction of $Sn^{4+}+H_2O \rightarrow Sn(OH)_4+4H^+$ and $Sn(OH)_4 \rightarrow SnO_2 \cdot xH_2O+(2-x)H_2O$ [19, 20]. When the polarization potential is increased beyond the transpassive potential, the current density of tinplate is suddenly increased due to the breakdown of passive film and the formation of corrosion pits on tinplate.

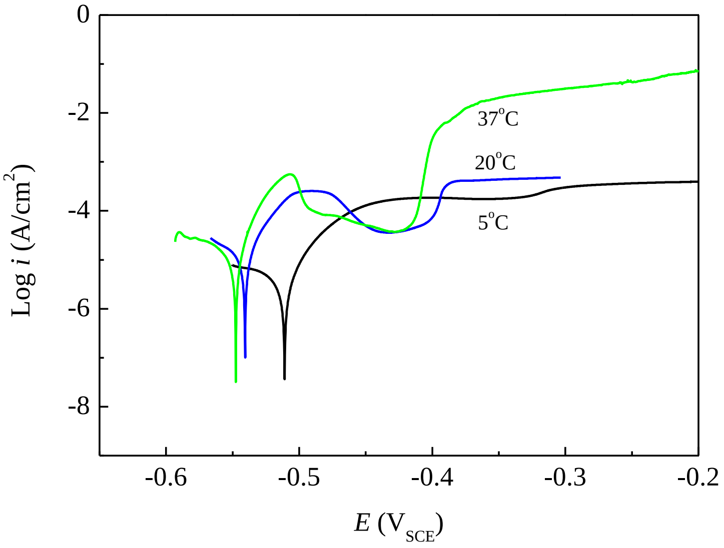

Figure 1. Polarization curves of tinplate in 0.1 mol/L citric acid solution at different temperatures

The calculated corrosion potential and corrosion current density of tinplate are listed in Table 1. Form Fig.1 and Table 1, it can be observed that the corrosion current density of tinplate at 20 °C and 37 °C is almost 2.0 and 2.5 times larger than that at 5 °C (Table 1), which means that the rise of storage temperature promotes the corrosion of tinplate in citric acid solution.

Table 1. Corrosion current density and potential of tinplate in 0.1 mol/L citric acid solution at different temperatures

T (°C)	E_{corr} (V_{SCE})	I_{corr} (μA/cm^2)
5	-0.511±0.010	4.842±0.520
20	-0.541±0.005	10.423±0.330
37	-0.547±0.006	11.995±0.460

3.2 EIS spectrum

Figure 2 is the EIS spectrum of tinplate in 0.1 mol/L citric acid solution at the temperature of 20 °C. At the immersion time less than 12 hours there are two time constants in EIS spectrum and the radius of capacitance arc is increased with the prolonging of immersion time (Fig.2a and Fig.2c), which indicating that the electrolyte had permeated the defects of tin coating and double layer capacitance was formed on the interface of steel substrate [8, 19]. The time constant at higher frequency is a result of tin coating interface capacitance Q_c and surface pore resistance of tin coating R_c, and the time constant at low frequency is a result of double layer capacitance Q_{dl} and charge transfer resistance R_{ct} of steel substrate. When the immersion time is longer than 12 hours, one time constant is observed in EIS spectrum which implies that the corrosion of tinplate is changed to the dissolution of steel substrate after the detachment or consumption of tin coating, and the radius of capacitance arc is decreased continually with the prolonging of immersion time (Fig.2b and Fig. 2d). Furthermore, there is an inductive arc observed at lower frequency in EIS spectrum, which means that the dissolved tin and iron ions were reacted with citric anions and then absorbed on tinplate surface [11, 12].

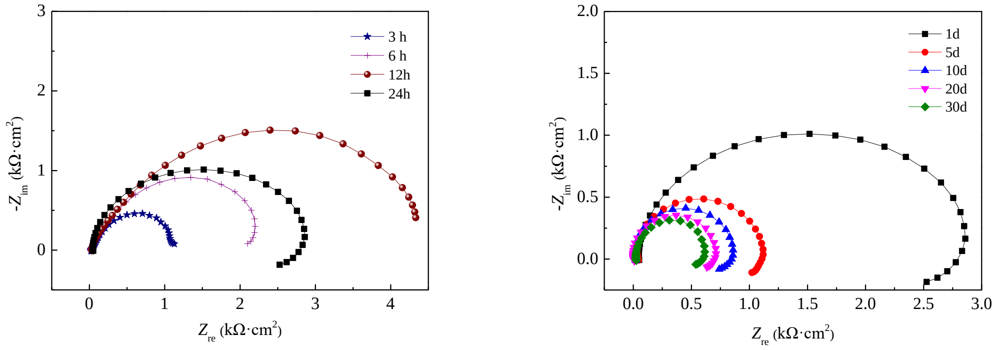

(a) Nyquist plot, 3-24 h (b) Nyquist plot, 1-30d

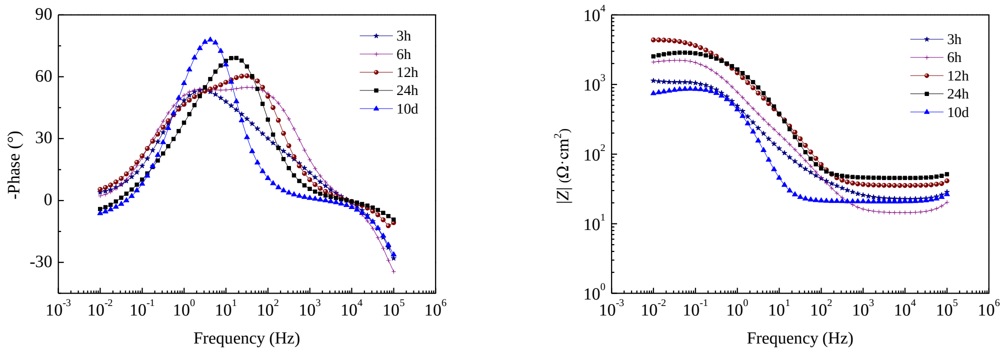

(c) Phase ~ *f* (d) |*Z*| ~ *f*

Figure 2. EIS spectrum of tinplate in 0.1 mol/L citric acid solution at 20 ^{o}C

EIS spectrum of tinplate in 0.1 mol/L citric acid solution at the temperature of 5 ^{o}C is shown in Figure 3. At the immersion time less than 24 hours, two time constants are also observed in the EIS spectrum of Fig.3a, and the radius of capacitance arc is increased with the immersion time (Fig.3a and Fig.3c). After that EIS spectrum is characterized with one time constant, and the radius of the capacitance arc is decreased continually with the prolonging of immersion time (Fig.3b and Fig. 3d), which are similar with the result at 20 ^{o}C. But the radius of capacitance arc at 5 ^{o}C is larger than that at 20 ^{o}C under the same immersion time, i. e. the corrosion resistance of tinplate at 5 ^{o}C is higher than that at 20 ^{o}C.

Figure 4 is the EIS spectrum of tinplate in 0.1 mol/L citric acid solution at the temperature of 37 ^{o}C. It can be seen from Fig.4 that EIS spectrum of tinplate is characterized by one time constant with a capacitance arc at higher frequency and an inductive arc at lower frequency, and the radius of capacitance arc at 37 ^{o}C is lower than that at 5 ^{o}C and 20 ^{o}C. At the initial immersion stage (3-12 hours), the radius of capacitance arc is slightly decreased with immersion time. When the immersion time is longer than

24 hours, the radius of capacitance arc is firstly increased and then reduced (Fig.4a and Fig. 4d). These results are probably related with the formation and detachment of corrosion products on the surface of tinplate.

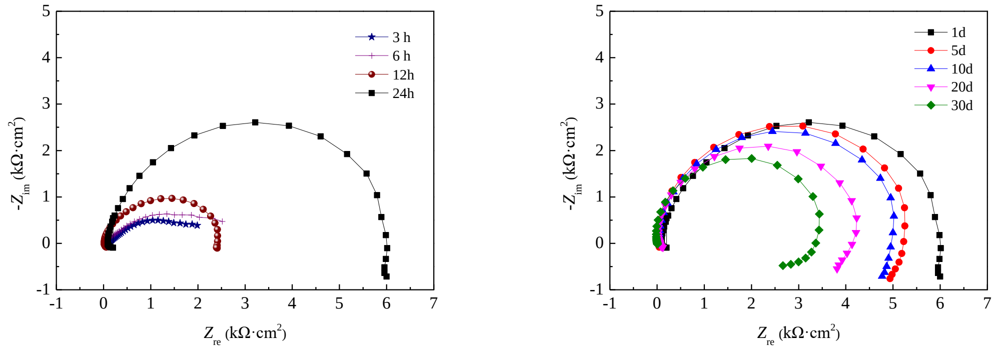

(a) Nyquist plot, 3-24 h (b) Nyquist plot, 1-30d

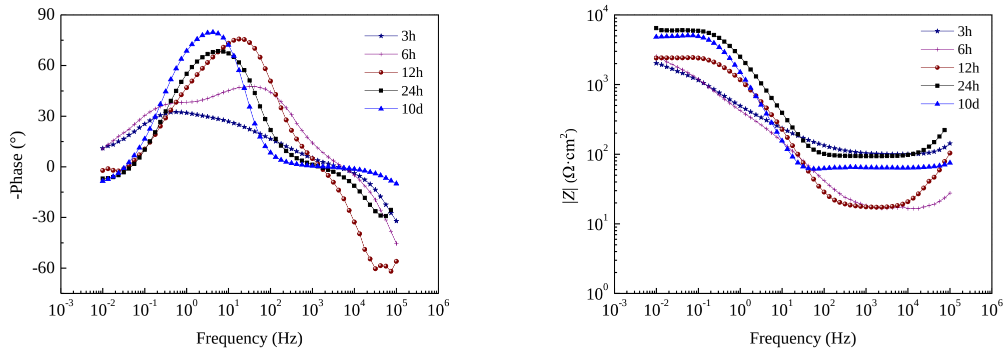

(c) Phase ~ *f* (d) |*Z*| ~ *f*

Figure 3. EIS spectrum of tinplate in 0.1 mol/L citric acid solution at 5 °C

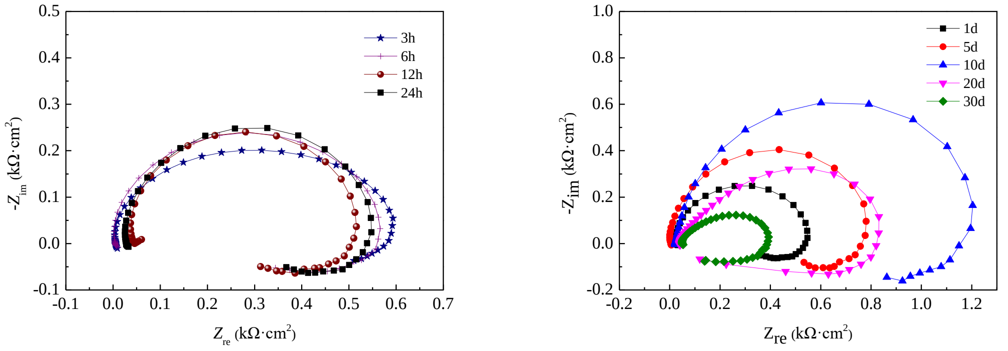

(a) Nyquist plot, 3-24 h (b) Nyquist plot, 1-30d

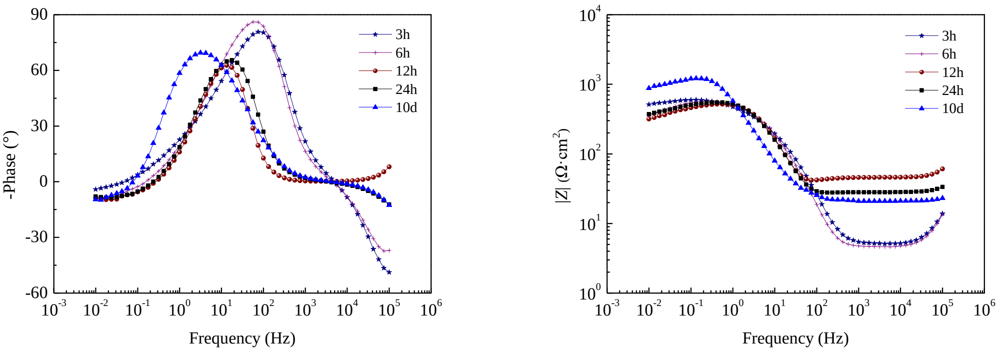

(c) Phase ~ *f* (d) |*Z*| ~ *f*

Figure 4. EIS spectrum of tinplate in 0.1 mol/L citric acid solution at 37 °C

For EIS spectrum in Figs. 2, 3 and 4, the equivalent circuits with two time constants (3-12 hours at 20 °C, and 3-24 hours at 5 °C) in Figure 5a and one time constant in Figure 5b were applied to analyze the experimental data, in which R_s is the electrolyte resistance, Q_c is the capacitance of tin coating, R_c is the resistance of tin coating, Q_{dl} is the double layer capacitance of steel substrate, and R_{ct} is the charge transfer resistance of steel substrate, *R* and *L* are the inductive parameters related with the absorbed corrosion products on tinplate surface [8, 21, 22, 23]. The fitting electrochemical parameters are calculated and listed in Table 2, and the variation of R_{ct} with the immersion time and temperature in citric acid solution is shown in Figure 6. It can be seen that the corrosion resistance of R_{ct} is firstly increased at the initial stage of immersion time (3-12 hours at 20 °C, and 3-24 hours at 5 °C) and then decreased obviously. The increasing of R_{ct} at the initial immersion stage is related with the formation of $Sn(OH)_4$ and SnO_2 film and the occurrence of FeSn intermetallic layer after depletion of pure tin coating on tinplate[23, 24], and the reduction of R_{ct} in the following stage is probably caused by consumption of tin coating and the corrosion of steel substrate. Under the same immersion time, tinplate has a lower corrosion resistance R_{ct} at higher temperature, which means that the promotion of storage temperature does enhance the corrosion rate of tinplate in citric acid solution.

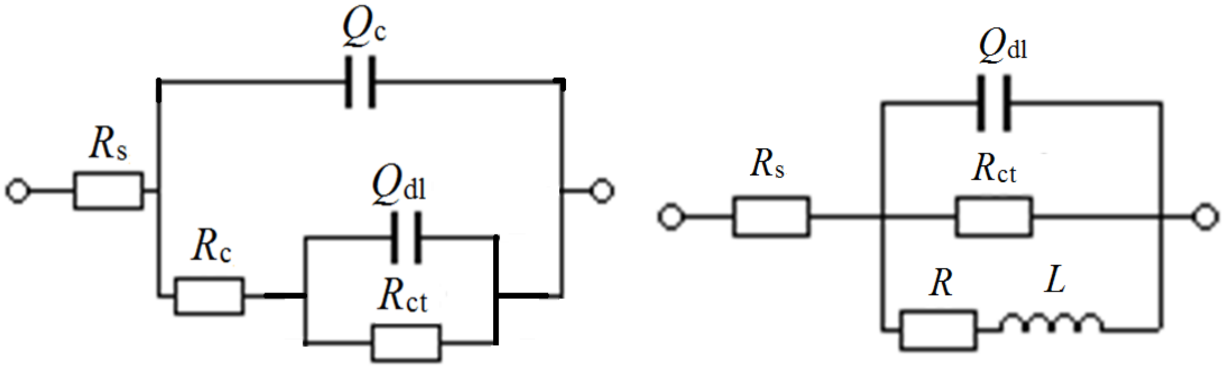

(a) two time constants (b) one time constants

Figure 5. Electrochemical equivalent circuits used for tinplate in 0.1 mol/L citric acid solution

Table 2. Fitting parameters for EIS spectrum of tinplate in 0.1 mol/L citric acid solution at different temperatures

T (℃)	t (hours)	R_s ($\Omega\cdot\mathrm{cm}^2$)	Q_c ($\mathrm{F}\cdot\mathrm{cm}^{-2}$)	R_c ($\Omega\cdot\mathrm{cm}^2$)	Q_dl ($\mathrm{F}\cdot\mathrm{cm}^{-2}$)	R_ct ($\Omega\cdot\mathrm{cm}^2$)	L ($\mathrm{H}\cdot\mathrm{cm}^2$)	R ($\Omega\cdot\mathrm{cm}^2$)
5	3	9.1	$1.3*10^{-4}$	154.00	$7.6*10^{-4}$	3007.0		
	6	16.4	$9.3*10^{-5}$	186.7	$3.0*10^{-4}$	3259.0		
	12	17.2	$1.0*10^{-4}$	236.1	$1.7*10^{-4}$	3816.0		
	24	10.9	$5.3*10^{-4}$	208.4	$7.9*10^{-5}$	5718.0	48.3	571.8
	120	10.6			$7.8*10^{-5}$	5279.0	120.7	517.1
	240	20.8			$1.0*10^{-4}$	4937.0	268.3	268.2
	480	22.0			$1.5*10^{-4}$	4161.0	280.8	329.1
	720	4.7			$2.0*10^{-4}$	3465.0	363.7	2383.6
20	3	24.0	$4.0*10^{-4}$	21.6	$1.6*10^{-4}$	1149.0		
	6	15.7	$1.2*10^{-4}$	92.7	$2.5*10^{-4}$	2248.0		
	12	35.5	$0.8*10^{-4}$	308.8	$1.6*10^{-4}$	3090.0		
	24	45.0			$3.2*10^{-4}$	2712.0	140.9	104.2
	120	38.8			$1.4*10^{-4}$	1942.0	298.3	271.2
	240	21.4			$3.4*10^{-4}$	1651.0	350.8	309.1
	480	9.0			$5.2*10^{-4}$	1225.0	369.7	273.6
	720	23.6			$8.9*10^{-5}$	836.2	139.9	254.2
37	3	7.6			$7.0*10^{-5}$	535.1	304.9	158.0
	6	6.8			$8.1*10^{-5}$	512.4	159.6	300.7
	12	5.8			$1.1*10^{-4}$	473.5	322.7	792.9
	24	8.2			$1.0*10^{-4}$	514.0	512.7	111.5
	120	5.8			$1.9*10^{-4}$	803.9	729.6	159.8
	240	8.5			$2.9*10^{-4}$	1370.0	907.9	256.2
	480	8.7			$2.8*10^{-4}$	886.4	505.4	716.8
	720	8.7			$1.5*10^{-4}$	344.1	189.4	168.7

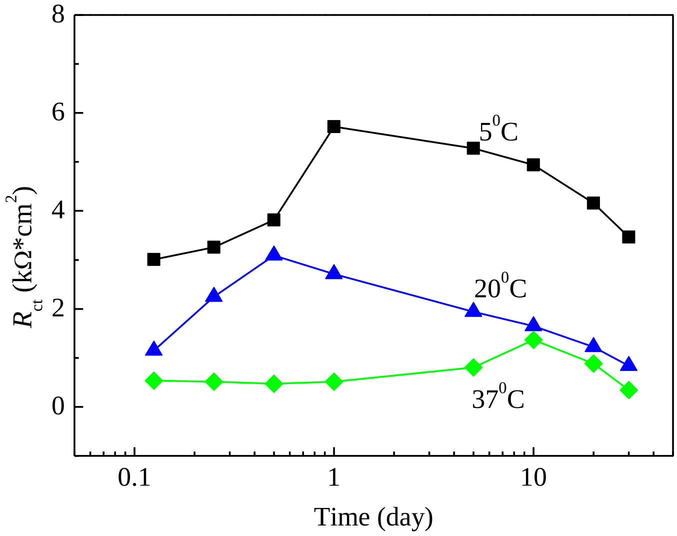

Figure 6. Variation of R_{ct} for tinplate in citric acid solution with immersion time at different temperatures

3.3 Surface morphology

The surface morphology of tinplate before and after immersion test in 0.1 mol/L citric acid solution at 20 °C is shown in Fig. 7, and the local magnified morphology and EDS spectrum of tinplate are shown in Fig.8. Before immersion, tinplate is in an uniform and smooth surface (Fig.7a and Fig.8a), and composed by 76.01 wt.% tin and small amount of iron element (Fig.8b). After 1 day's immersion, there are corrosion pits occurred on the tinplate surface (Fig.7b).

Meanwhile, FeSn intermetallic layer with cross arranged columnar structures, which is formed between the interface of tin coating and steel substrate during the reflowing process, was appeared (Fig.8c) [7, 14, 25, 26], and the tin content of corroded surface is decreased to 36.64 wt. % tin. These results mean that the pure tin coating on the steel substrate is almost corroded away after 1 day's immersion. With the further immersion in citric acid solution, FeSn intermetallic layer on the tinplate is gradually dissolved (Fig.7c). Finally, the steel substrate underneath the tin coating is completely exposed in the solution at the immersion time of 30 days (Fig.7d).

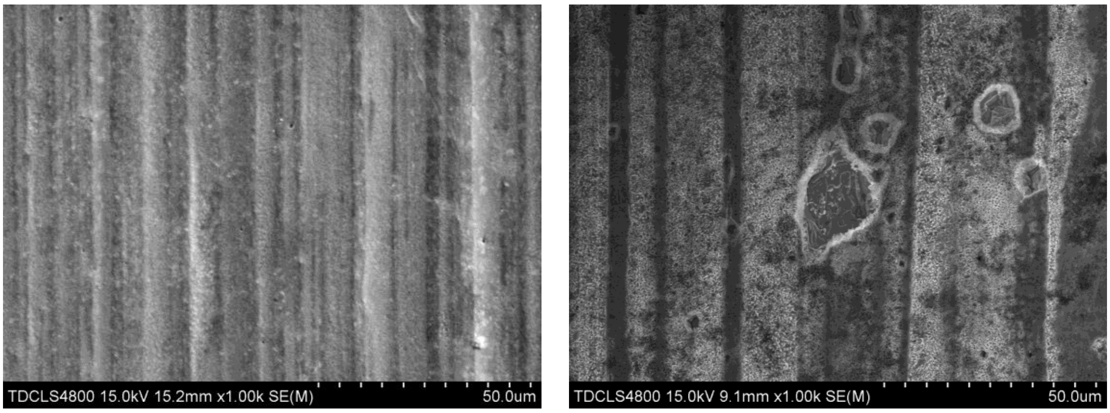

(a) before immersion (b) immersion time of 1 d

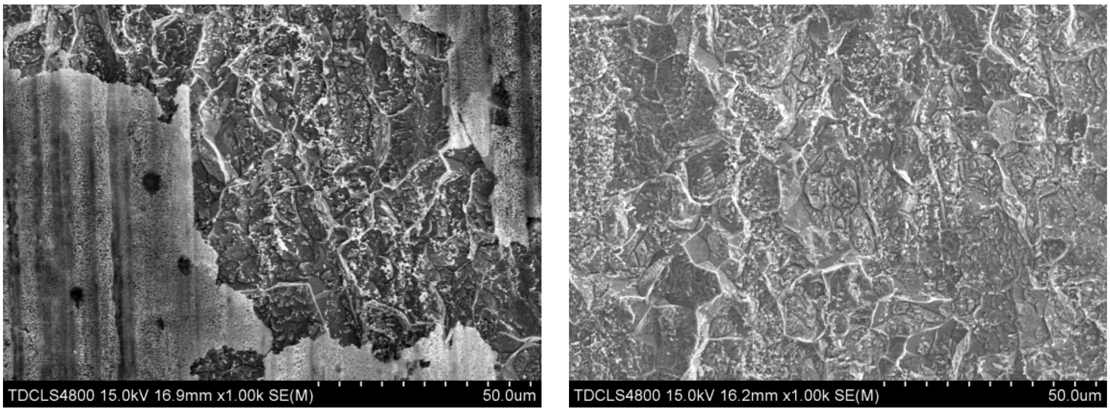

(c) immersion time of 10 d (d) immersion time of 30 d

Figure 7. Surface morphology of tinplate before and after immersion test in citric acid solution at 20 ^{o}C

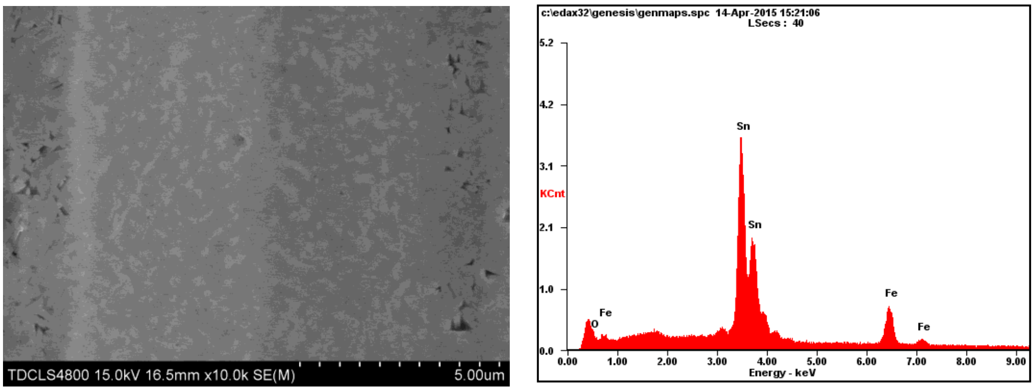

(a) local morphology of Fig.7a (b) EDS spectrum of Fig.8a

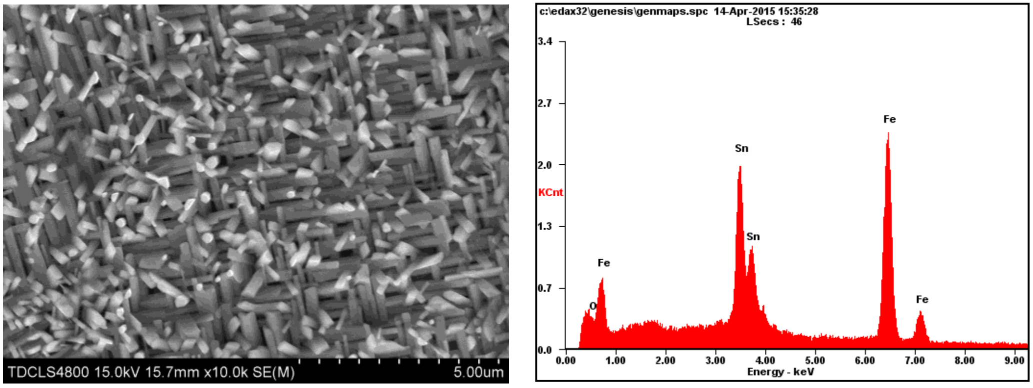

(c) local morphology of Fig.7b (d) EDS spectrum of Fig.8c

Figure 8. Surface morphology and EDS spectrum of tinplate before and after immersion

Fig.9 and Fig.10 are the surface morphologies of tinplate after immersion test at 5 ^{o}C and 37 ^{o}C. At the temperature of 5 ^{o}C, there are corrosion pits observed on the tinplate, and the density and size of corrosion pits are increased with the prolonging of immersion time (Fig. 9a and Fig.9b). After 30 days' immersion, the tin coating is begun to peel off (Fig.9c). At the temperature of 37 ^{o}C, there are also corrosion pits occurred on the tinplate surface after 1 day's immersion (Fig.10a). Under the immersion time of 10 days, half of the tin coating has been peeled off (Fig.10b). When the immersion time is increased to 30 days, corrosion pits are formed on the steel substrate (Fig.10c).

From the above evolution of surface morphology in Figs 7, 9 and 10, it also can be observed that tinplate has a higher corrosion rate in citric acid solution under higher temperature.

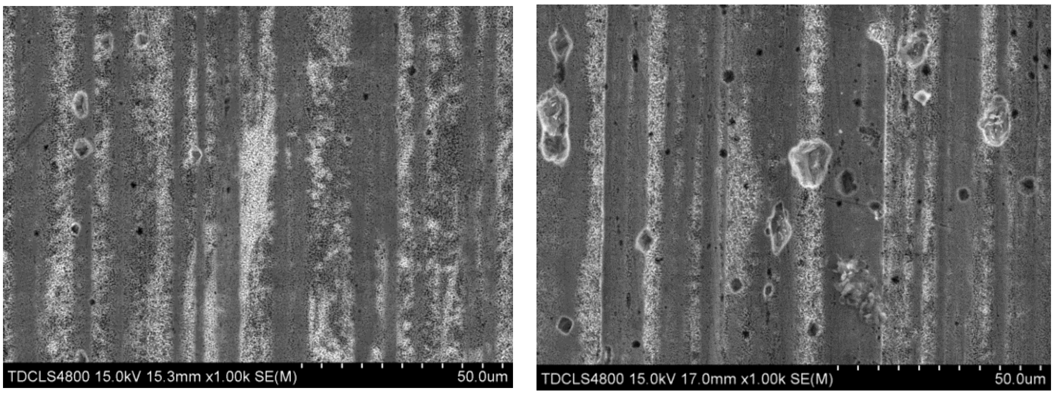

(a) immersion time of 1 d (b) immersion time of 10 d

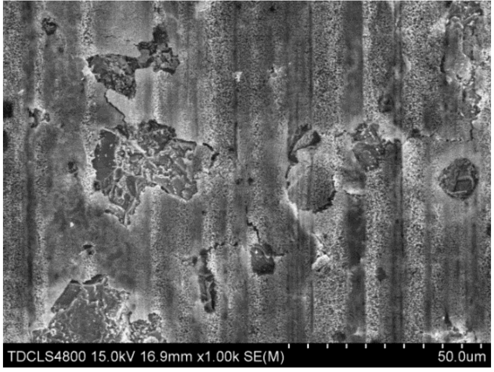

(c) immersion time of 30 d

Figure 9. Surface morphology of tinplate after immersion in citric acid solution at 5 ^{o}C

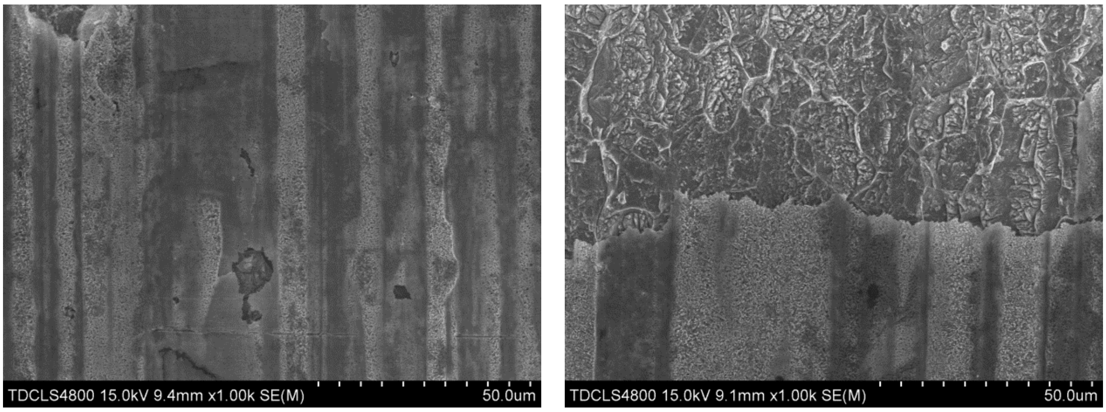

(a) immersion time of 1 d (b) immersion time of 10 d

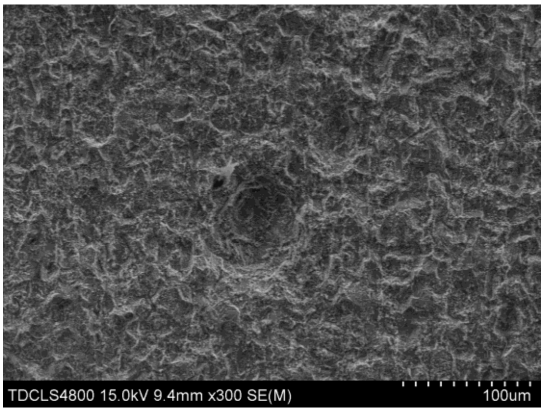

(c) immersion time of 30 d

Figure 10. Surface morphology of tinplate before and after immersion test in citric acid solution at 37 °C

3.4 ICP analysis

The concentration of iron and tin ions dissolved in citric acid solution at different temperatures was determined and shown in Fig.11. It can be found that the concentration of Fe and Sn elements in solution under the same immersion time is increased obviously with the increasing of testing temperature, which means that the increased temperature promotes the corrosion process of tinplate in citric acid solution.

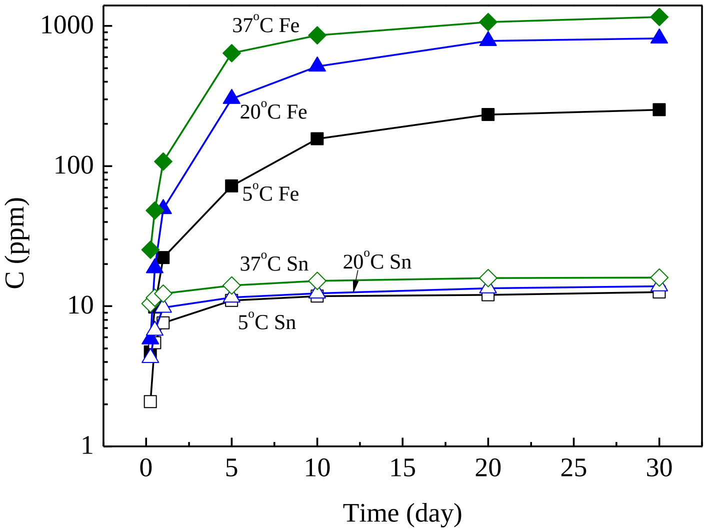

Figure 11. Concentration of Fe and Sn ions in citric acid solution at different temperature

At the immersion time less than 24 hours, the concentration of Fe and Sn elements is increased almost linearly with the immersion time, which indicating the codissolution of tin and iron elements in solution and corresponding the two time constants in EIS spectrum in Fig.2a and Fig.3a. After the immersion time longer than 1 day, the dissolution rate of Fe and Sn elements in solution is reduced, but the concentration of Fe element is still increased rapidly, and almost two orders higher than that of Sn element under the same immersion time. This result implies that the corrosion of tinplate after 1 day's immersion is dominated by the dissolution of steel substrate, which is agreed with the one time constant in EIS spectrum in Fig.2b, Fig.3b and Fig.4.

4. DISCUSSION

From the results of Figs. 1 to 4, Fig.6 and Fig.11, it can be deduced that under higher storage temperature tinplate has a higher corrosion current density, lower polarization resistance and higher Fe and Sn content in citric acid solution. These experimental data proved that the corrosion of tinplate in citric acid solution will be accelerated by the promotion of storage temperature.

4.1 Activation energy

In order to analyze the influence of temperature on the corrosion behavior of tinplate, Arrhenius equation $i = \mathrm{A}\mathrm{e}^{-\frac{E_\mathrm{a}}{R'T}}$ [27] and Stern-Geary equation $i = B/R\mathrm{p}$ [28] were applied to determine the activation energy of tinplate in citric acid solution, in which E_a is the activation energy of corrosion process (J/mol), *R'* is the universal gas constant of 8.314J/(mol·K), *T* is the testing temperature (K), *A* and *B* are the preexponential factor and Stern-Geary constant. Based on the resistance of R_ct in Table 2 and Fig.6, the activation energy of tinplate can be calculated by the slope of following equation [29]:

$$\log(1/R_\mathrm{ct})=\log(A')-\frac{E_\mathrm{a}}{2.303R'T} \quad (1)$$

Where *A*'=*A*/*B*.

The dependence of log(1/R_ct) for tinplate in citric acid solution on 1/*T* is shown in Fig.12, and the activation energy of tinplate at different immersion time is calculated and plotted in Fig.13. At the immersion time less than 24 hours, the activation energy of tinplate is kept in a higher value of 38.93~57.27 kJ/mol, and then decreased obviously with immersion time. This high activation energy is probably related with the physical protection effect of passivated tin coating, FeSn intermetallic layer (Fig.8c) and absorbed corrosion products formed on the tinplate, which is agreed with the two time constants in EIS spectrum in Fig.2a and Fig.3a, the increasing R_ct in Fig.6 and the codissolution of tin and iron in Fig.11. With the immersion time prolonged to 10 to 20 days, the activation energy of tinplate is reduced to a lower value of 28.57-34.51 kJ/mol, which means that the corrosion of tinplate is changed to the dissolution of steel substrate after the consumption of tin coating (Figs.7, 9 and 10). When the immersion time is extended to 30 days, the activation energy is again increased to a higher value of 51.66kJ/mol because of the absorbed corrosion products on the steel substrate.

4.2 Corrosion process

From the above experimental results in Figs. 2-4, Fig.6, Fig.11, Fig.13 and the evolution of corroded surface morphology in Figs. 7-10, the corrosion process of tinplate in citric acid solution could be divided into two stages. At the initial stage with the immersion time less than 24 hours at 5 °C or 12 hours at 20 °C or 3 hours at 37 °C, citric acid solution is directly contacted with tin coating, and also could be reacted with the steel substrate by permeating the defects of tin coating. So the corrosion of tinplate at this stage is by the codissolution of tin and iron in citric acid solution (Fig.11), and there are two time constants in EIS spectrum (Fig.2a and Fig.3a). With the immersion time longer that 1 day, the tin coating including FeSn intermetallic layer outside the steel substrate is gradually corroded away or detached by the corrosion products between the tin coating and steel substrate (Fig.7c and Fig.9b), the steel substrate is almost totally begun to contact with citric acid solution (Fig.7d). And thus the corrosion of tinplate is mainly by the dissolution of steel substrate (Fig.11), and EIS spectrum of tinplate is changed to one time constant (Fig.2b, Fig.3b and Fig.4b).

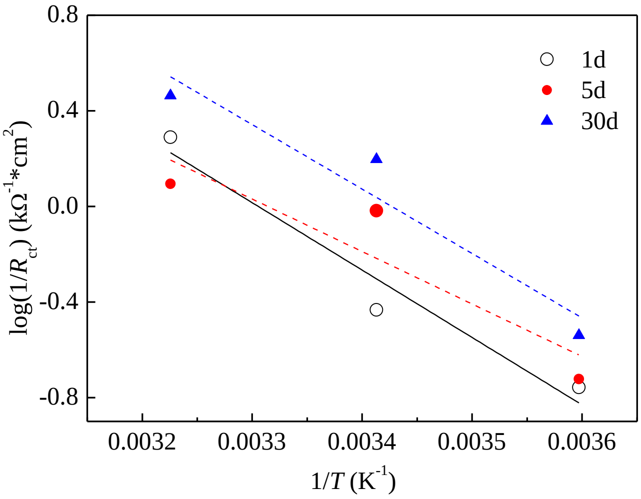

Figure 12. Dependence of log(1/R_{ct}) for tinplate in citric acid solution on 1/T

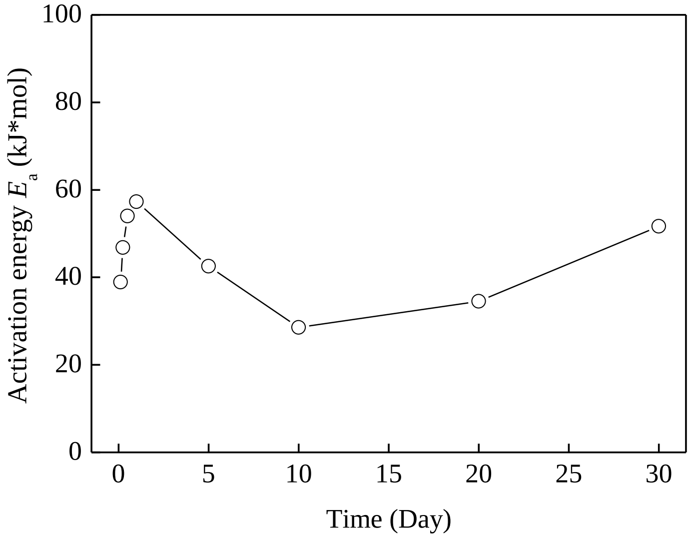

Figure 13. Activation energy of tinplate in citric acid solution at different immersion time

Although two corrosion stages could be classified for tinplate in citric acid solution under different storage temperature, the corrosion rate and duration of every corrosion stage are varied with storage temperature. With the increasing of temperature, tinplate has a higher corrosion rate (Table 1), lower corrosion resistance (Fig.6) and higher iron and tin dissolution content in citric acid solution (Fig.11), and the duration from the codissolution of tin and iron (initial stage) to the steel dissolution (second stage) is decreased (Fig.6, Fig.7, Fig.9 and Fig.10). These results also proved that the increasing storage temperature does accelerate the corrosion process of tinplate in citric acid solution.

5. CONCLUSIONS

(1) With the increasing of storage temperature from 5 °C to 37 °C, tinplate has a more negative corrosion potential, higher corrosion current density, lower initiating passive potential and lower transpassive potential in citric acid solution.

(2) At the initial immersion stage, the corrosion of tinplate is by the codissolution of tin and iron, and there are two time constants in EIS spectrum. With the prolonging of immersion time, there is only one time constant observed in EIS spectrum, and tinplate is changed to the dissolution of steel substrate.

(3) The corrosion process of tinplate in citric acid solution can be classified into two stages, in which the initial stage of corrosion has a higher activation energy of 38.93~57.27 kJ/mol, whereas the activation energy in the following stage is firstly decreased to a lower value of 28.57-34.51 kJ/mol and then increased again.

ACKNOWLEDGMENTS
This work was supported by National Natural Science Foundation of China (No. 51771133); National Basic Research Program of China (No. 2014CB046801) and Independent Innovation Fund Cooperation Project between Tianjin University and Qinghai University for Nationalities (No.1706).

References

1. D. Y. Fantis, A. Yfantis, B. Tzalas, D. Schmeisser, *Corrosion*, 56 (2000) 700.
2. G. F. Cui, J. H. Wang, N. Li, X. Q. Huang, *Mater. Chem. & Phys.*, 97 (2006)488.
3. S. Blunden, T. Wallace, *Food & Chem. Toxicol.*, 41 (2003) 1651.
4. A. V. Pournaras, M. I. Podromidis, A. P. Katsoulidis, A. V. Badeka, D. Georgantelis, M. G. Kontominaset, *J. Food Eng.*, 86 (2008) 460.
5. P. W. Board, R. V. Holland, R. J. Steele, *Brit. Corros. J.*, 7 (1972)87.
6. R. Catala, J. M. Cabanes, J. M. Bastidas, *Corros. Sci.*, 40(1998) 1455.
7. Y. Che, Z. W. Han, B. Luo, D. H. Xia, J. B. Shi, Z. M. Gao, J. H. Wang, *Int. J. Electrochem Sci.*, 7 (2012) 9997.
8. D. H. Xia, S. Z. Song, J. H. Wang, H. C. Bi, B. Zhang, *Trans. Nonferrous Met. Soc. China*, 22 (2012) 717.
9. D. Álvarez, A. Collazo, X. R. Novoa, C. Petrz, *Prog. Org. Coat.*, 77 (2014) 2066.
10. K. K. Baldin, S. R. Kunst, V. R. Beltramil, T. M. Lemos, M. C. Quevedo, A.C. Bastos, G. S. Marioferreira, P. R. R. Santos, V. H. V. Sarmento, C. F. Malfatti, *Thin Solid Films*, 600 (2016) 146.
11. M. Jafarian, F. Gobal, I. Danaee, R. Biabani, M. G. Mahjani, *Electrochim. Acta*, 53 (2008) 4528.
12. D. J. Zhou, J. H. Wang, Y. Gao, L. Zhang, *Int. J. Electrochem. Sci.*, 12(2017)639.

13. E. Zumelzu, C. Cabezas, F. Delgado, *J. Mater. Process. Tech.*, 152 (2004) 384.
14. E. H. A. Addi, I. Zaanoun, A. A. Addi, A. Found, L. Bazzi, A. Outzouighit, *Int. J. Electrochem. Sci.*, 8 (2013) 7842.
15. D. H. Xia, S. Z. Song, J. H. Wang, H. C. Bi, Z. W. Han, *Acta Phys.-Chim. Sin.*, 28 (2012) 121.
16. K. Wang, J. H. Wang, H. H. Wang, C. W. Fu, D. H. Xia, X. Zheng, L. H. Dang, J. B. Shi, *J. Cent. South Univ. Tech.*, 20(2014)76.
17. D. H. Calloway, J. J. Mcmullen, *Am. J. Clin. Nutr.*, 18(1966)1.
18. D. J. Zhou, J. H. Wang, Y. Gao, L. Zhang, *Int. J. Electrochem Sci.*, 12(2017)192.
19. S. S. Abdel Rehim, S. M. Sayyah, M. M. El Deeb, *Mater. Chem. & Phys.*, 80(2003)696.
20. N. Mora, E. Cano, J. L. Polo, J. M. Puente, J. M. Bastidas, *Corros. Sci.*, 46(2004) 563.
21. J. H. Wang, C. W. Fu, Z. M. Gao, D. H. Xia, *Trans. Tianjin Univ.*, 19(2013)235.
22. X. H. Wang, J. H. Wang, C. W. Fu, *Trans. Nonferrous Met. Soc. China*, 24 (2014) 3907.
23. X. Q. Huang, F. J. Lang, Y. Mai, Y. Chen, Z. Zhang, J. Q. Zhang, *Trans. Nonferrous Met. Soc. China*, 24 (2014)1978.
24. N. Wint, S. Geary, H. N. Mcmurray, G. Williams, A.Vooys, *J. Electrochem. Soc.*, 162(2015)C775.
25. M. J. L. Gines, G. J. Benítez, W. Egli, J. L. Zubimendi, T. Pérez, *Plat. & Surf. Finish.*, 90(2003)44.
26. E. Zumelzu, C. Cabezas, A. Vera, *Scanning*, 25(2003)34.
27. P. W. Atkins, *Physical Chemistry*, 5th ed., Oxford University Press, Oxford, (1994) 877.
28. N. Perez, *Electrochemistry and Corrosion Science*, Kluwer Academic Publishers, Boston, (2004) 85.
29. R. M. Elsherif, K. M. Ismail, W. A. Badawy, *Electrochim. Acta*, 49(2004)5139.